Electronic Supplementary Material

Photocatalytic syngas synthesis from CO_2 and H_2O using ultrafine CeO_2-decorated layered double hydroxide nanosheets under visible-light up to 600 nm

Ling Tan*, Kipkorir Peter*, Jing Ren, Baoyang Du, Xiaojie Hao, Yufei Zhao (✉), Yu-Fei Song (✉)

State Key Laboratory of Chemical Resource Engineering, Beijing University of Chemical Technology, Beijing 100029, China

E-mails: zhaoyufei@mail.buct.edu.cn (Zhao Y); songyf@mail.buct.edu.cn (Song Y)

Table S1. BET surface areas of LDH, Ce-0.15, Ce-0.20 and Ce-0.40

sample	BET surface area/($m^2 \cdot g^{-1}$)
LDH	108.84
Ce-0.15	116.88
Ce-0.20	110.74
Ce-0.40	58.92

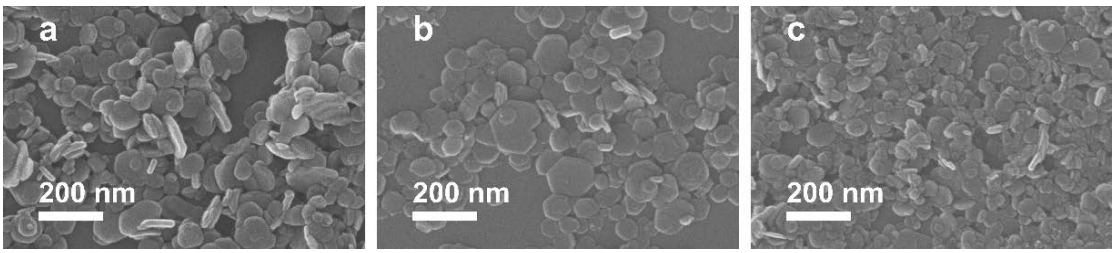

Figure S1. SEM images of (a) LDH (b) Ce-0.15 and (c) Ce-0.40.

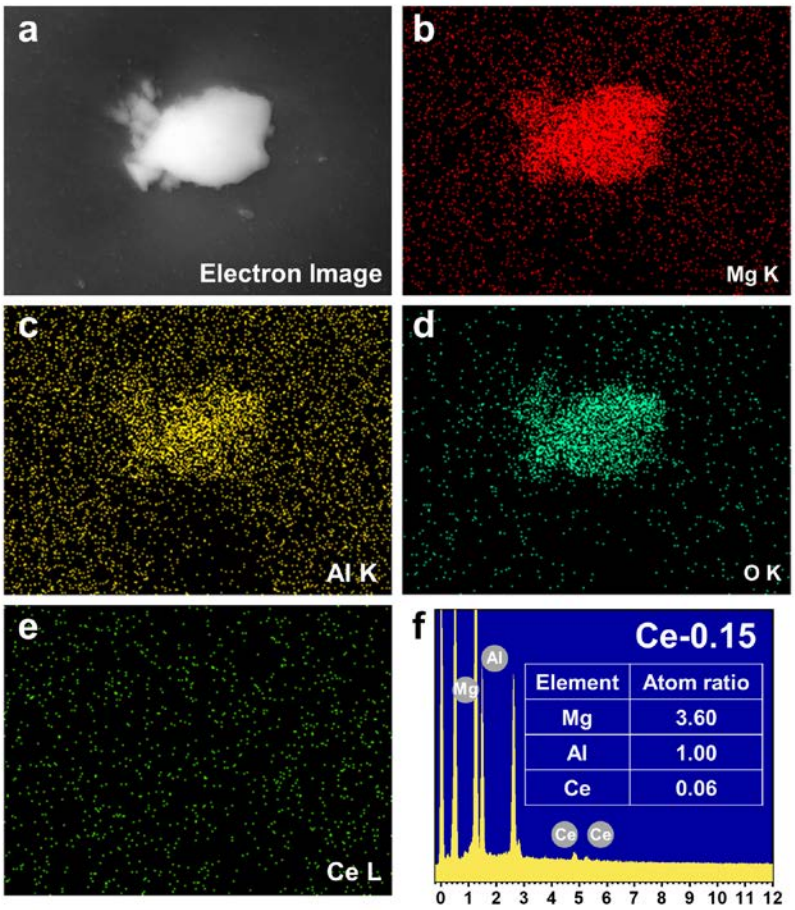

Figure S2. (a) SEM image of Ce-0.15; Energy-dispersive X-ray (EDS) elemental mapping of Ce-0.15 for (b) Mg, (c) Al, (d) O and (e) Ce, respectively; (f) EDS spectroscopy of Ce-0.15.

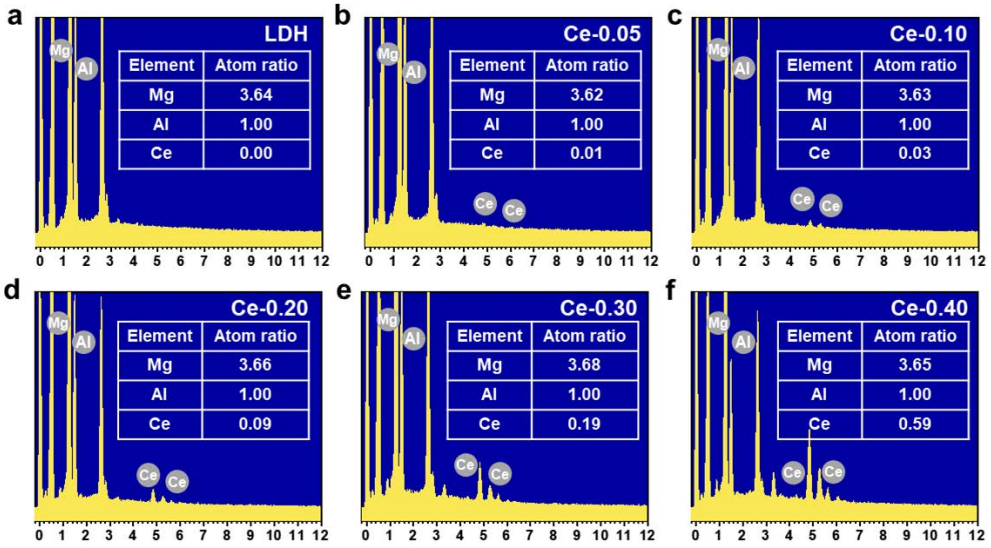

Figure S3. Energy-dispersive X-ray spectroscopy of (a) LDH, (b) Ce-0.05, (c) Ce-0.10, (d) Ce-0.20, (e) Ce-0.30 and (f) Ce-0.40, respectively.

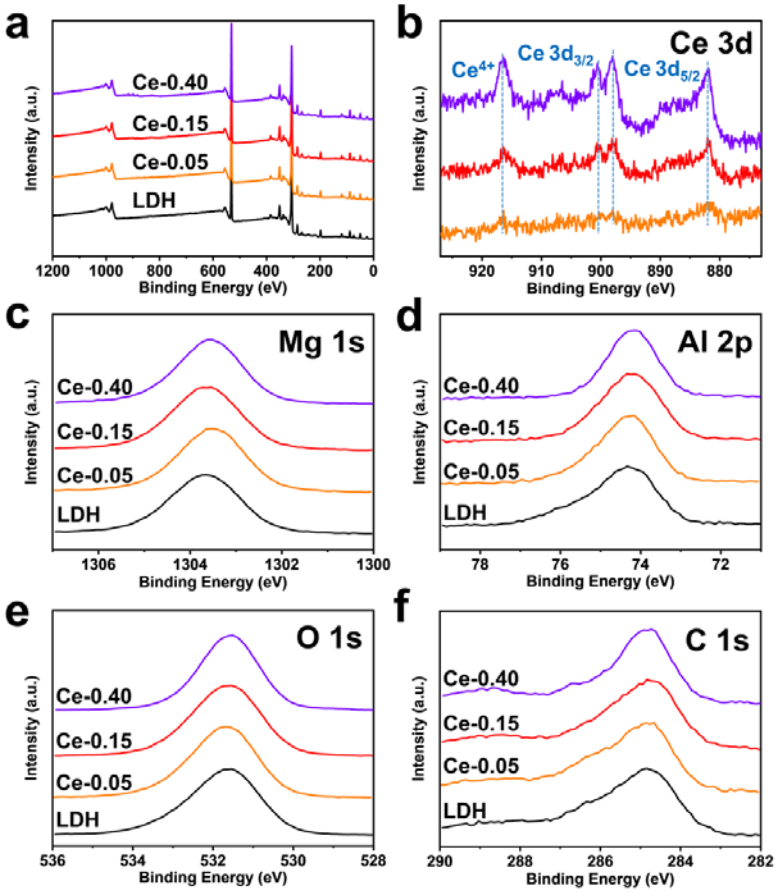

Figure S4. XPS (a) survey spectra and (b) Ce 3d spectra for LDH, Ce-0.05, Ce-0.15 and Ce-0.40.

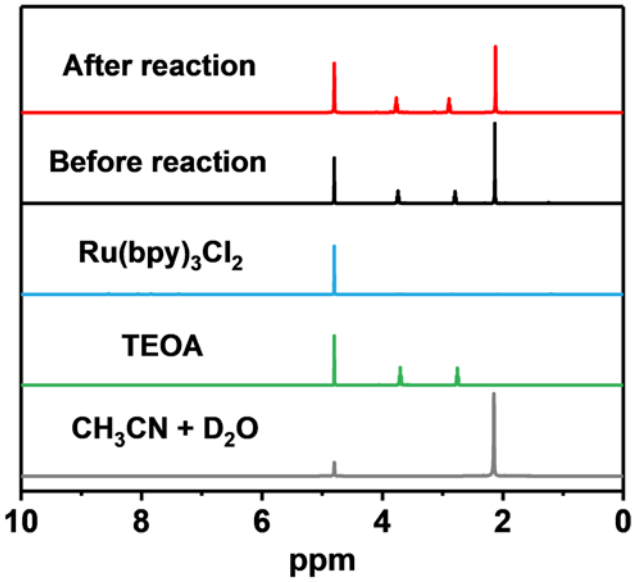

Figure S5. ^{1}H-NMR spectra of CH_3CN, TEOA, $Ru(bpy)_3Cl_2 \cdot 6H_2O$ and liquid sample, taken from the reaction system (irradiating with $\lambda > 400$ nm for 1 h).

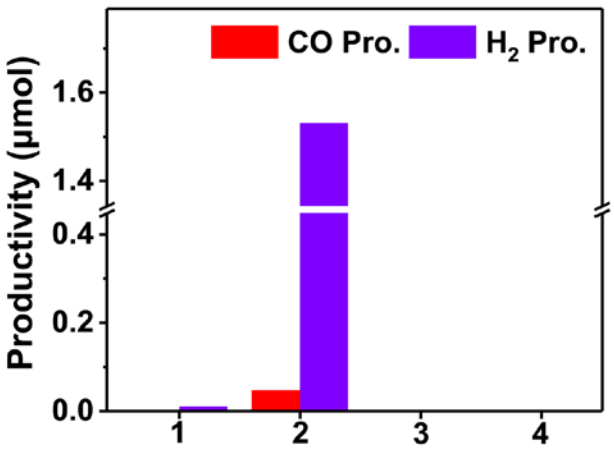

Figure S6. The productivity of catalyst under control reaction conditions experiments, note: 1. Ar atmosphere, 2. Without Ce-0.15, 3. Without $Ru(bpy)_3Cl_2$, 4. In dark.

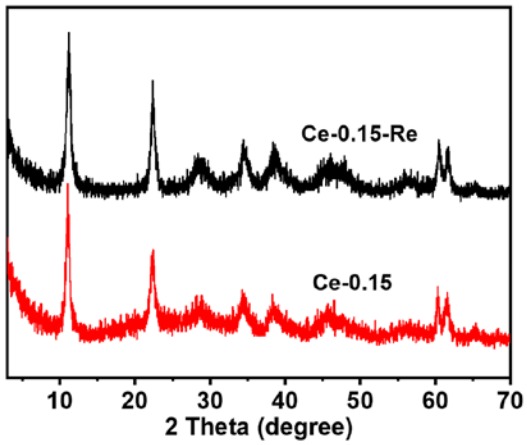

Figure S7. XRD patterns of Ce-0.15 and the recycled Ce-0.15 (denoted as Ce-0.15-Re).

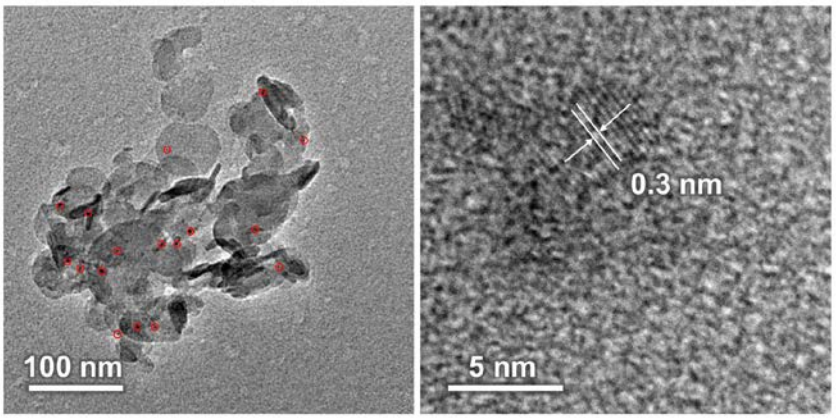

Figure S8. (a) TEM image and (b) HRTEM image of recycled Ce-0.15.

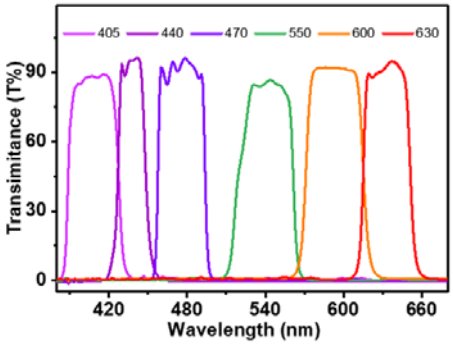

Figure S9. The monochromatic light at different wavelength adapted from our previous work.[1]

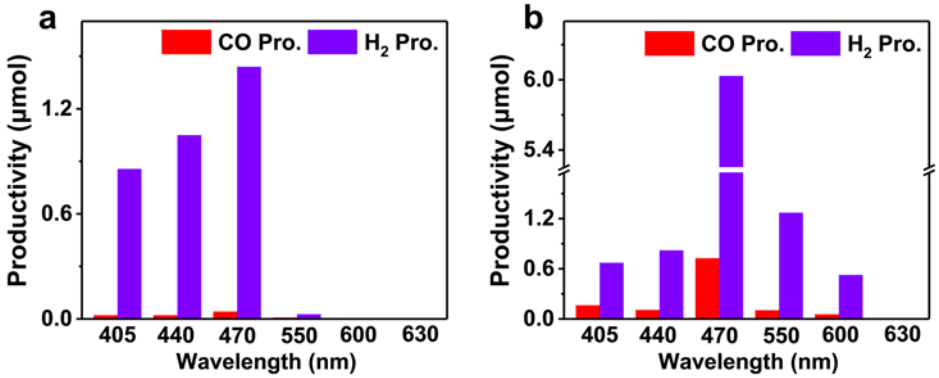

Figure S10. The productivity of (a) LDH and (b) Ce-0.15 in CO_2PR under different cut-off filter light irradiation.

The External Quantum Efficiency (EQE) values of CO was calculated using the equation as reported:[2]

$$\mathrm{EQE}(\%) = \frac{2n \times N_A \times h \times c}{t_{irr} \times \lambda \times I \times A} \times 100$$

Where n is the amount of CO produced per time, N_A is Avogadro's constant, h is the Planck constant, c is the speed of light, t_{irr} is the irradiation time, λ is the irradiation wavelength, I is the irradiation intensity and A is the irradiated area. So, the EQE values of CO under different wavelength irradiation was shown as Table S2.

Table S2. The External Quantum Efficiency (EQE) values of CO under different wavelength irradiation by LDH and Ce-0.15

Sample	405 nm	470 nm	550 nm	600 nm
LDH (%)	0.05	0.04	0.07	0
Ce-0.15 (%)	0.43	1.45	0.16	0.05

Table S3. Comparison of photocatalytic CO_2 reduction performance for various photocatalysts in this work and in previous literature

	photocatalyst	photosensitizer co-catalyst	sacrificial agent	solvent	light source	evolution rate of major product (μmol g^{-1} h^{-1})	reference
1	Ce-0.15	$Ru(bpy)_3Cl_2·6H_2O$	TEOA	MeCN-H_2O (3:1 v/v)	300 W Xe (λ = 600 nm)	**CO: 5 (8.7%) H_2: 52 (91.3%)**	**This work**
2	Pd/CoAl-7.57	$Ru(bpy)_3Cl_2·6H_2O$	TEOA	MeCN-H_2O (3:1 v/v)	300 W Xe (λ > 600 nm)	CO: 4.1 (43.2%) H_2: 5.4 (56.8%)	JEC, 2020, 46, 1[3]
3	CoAl-LDH	$Ru(bpy)_3Cl_2·6H_2O$	TEOA	MeCN-H_2O (3:1 v/v)	300 W Xe (λ = 600 nm)	CO: 43730 (55.8%) H_2: (44.2%)	IECR, 2020, 59, 5848[4]
4	$ZnIn_2S_4$−In_2O_3	$CoCl_2$ 2’2-bipyridine	TEOA	MeCN-H_2O (3:2 v/v)	300 W Xe (λ > 400 nm)	CO: 3075 (~75%) H_2: ~800 (~25%)	JACS, 2018, 140, 5037[5]
5	Co-G nanosheet	$Ru(bpy)_3Cl_2·6H_2O$	TEOA	MeCN-H_2O (3:1 v/v)	300 W Xe (λ > 420 nm)	CO: (79.4%) H_2: (20.6%)	Adv. Mater. 2018, 1704624[6]
6	Ni MOLs (Ni MOF monolayers)	$Ru(bpy)_3Cl_2·6H_2O$	TEOA	MeCN-H_2O (3:2 v/v)	5 W LED (λ > 400 nm)	CO: 12500 (97.8%) H_2: 280 (2.2%)	Angew, 2018, 57,16811[7]
7	MAF-X27*l*-OH	$Ru(bpy)_3Cl_2·6H_2O$	TEOA	MeCN-H_2O (4:1 v/v)	LED (λ > 420 nm)	CO: 45 μmol (98.3%) H_2: 0.8 μmol (1.7%)	JACS, 2018, 140, 38[8]
8	Dye/TiO_2/Re(I): Co(III) complex (9:1)	dye	BIH	DMF-H_2O (4:1 v/v)	60 W LED (λ > 400 nm)	CO: (76.9%) H_2: (23.1%)	Angew, 2017, 56, 976[9]
9	In_2S_3-$CdIn_2S_4$	$Co(bpy)_3^{2+}$	TEOA	MeCN-H_2O (3:2 v/v)	300 W Xe (λ > 400 nm)	CO: 825 (70.2%) H_2:~350 (29.8%）	JACS, 2017, 139, 17305[10]
10	Co_3O_4-400	$Ru(bpy)_3Cl_2·6H_2O$	TEOA	MeCN-H_2O (3:1 v/v)	300 W Xe (λ > 420 nm)	CO: 2003 (77.1%) H_2: 595 (22.9%)	Adv. Mater. 2016, 28, 6485[11]
11	C doped BN	$CoCl_2$ 2’2-bipyridine	TEOA	MeCN-H_2O (2:1 v/v)	300 W Xe (λ > 420 nm)	CO: 9.3 (76.2%) H_2: 2.9 (23.8%)	Nature Commun., 2015, 6, 7698[12]

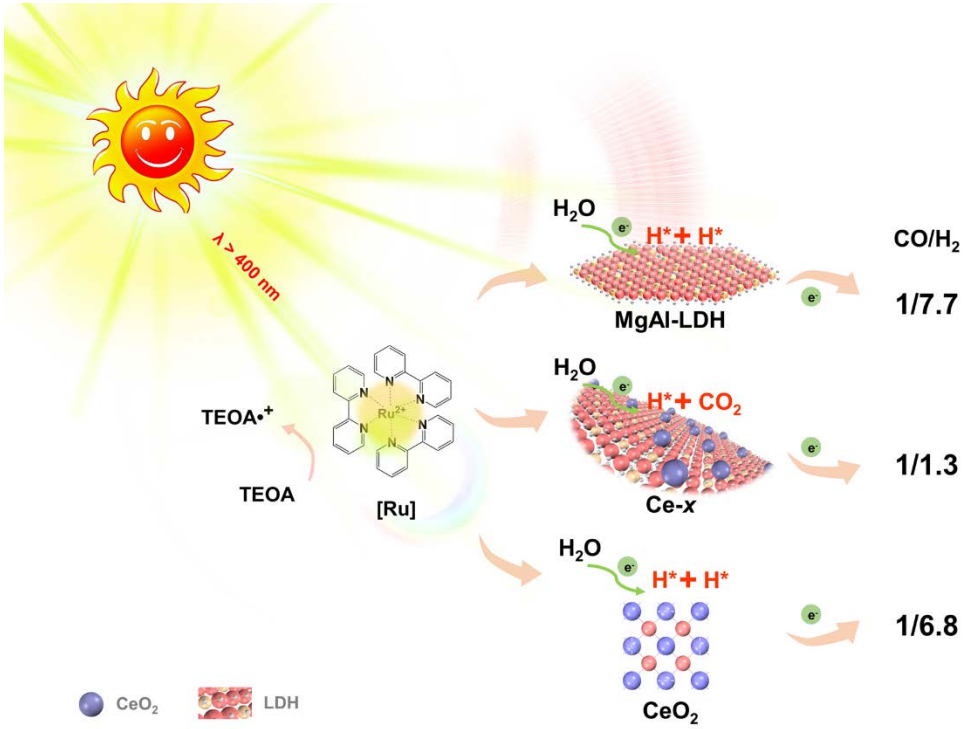

Scheme S1. The mechanism schematic of the photocatalytic CO_2 on LDH, Ce-*x* and CeO_2, respectively.

Reference

1. Tan L, Xu S M, Wang Z, Xu Y, Wang X, Hao X, Bai S, Ning C, Wang Y, Zhang W, et al. Highly selective photoreduction of CO_2 with suppressing H_2 evolution over monolayer layered double hydroxide under irradiation above 600 nm. Angewandte Chemie International Edition, 2019, 58: 11860-11867
2. Kuehnel M F, Creissen C E, Sahm C D, Wielend D, Schlosser A, Orchard K L, Reisner E. ZnSe nanorods as visible‐light absorbers for photocatalytic and photoelectrochemical H2 evolution in water. Angewandte Chemie International Edition, 2019, 58(15): 5059-5063
3. Wang X, Wang Z, Bai Y, Tan L, Xu Y, Hao X, Wang J, Mahadi A H, Zhao Y, Zheng L, et al. Tuning the selectivity of photoreduction of CO_2 to syngas over Pd/layered double hydroxide nanosheets under visible-light up to 600 nm. Journal of Energy Chemistry, 2020, 46: 1-7
4. Bai S, Wang Z, Tan L, Waterhouse G I N, Zhao Y, Song Y F. 600 nm irradiation-induced efficient photocatalytic CO_2 reduction by ultrathin layered double hydroxide nanosheets. Industrial & Engineering Chemistry Research, 2020, 59(13): 5848-5857
5. Wang S B, Guan B Y, Lou X W. Construction of $ZnIn_2S_4$-In_2O_3 hierarchical tubular heterostructures for efficient CO_2 photoreduction. Journal of the American Chemical Society, 2018, 140: 5037-5040
6. Gao C, Chen S, Wang Y, Wang J, Zheng X, Zhu J, Song L, Zhang W, Xiong Y. Heterogeneous single-atom catalyst for visible-light-driven high-turnover CO_2 reduction: the role of electron transfer. Advanced Materials, 2018, 30(13): 1704624
7. Han B, Ou X, Deng Z, Song Y, Tian C, Deng H, Xu Y J, Lin Z. Nickel metal-organic frameworks monolayers for photoreduction of diluted CO_2: metal-node-dependent activity and selectivity. Angewandte Chemie International Edition, 2018, 57: 16811-16815
8. Wang Y, Huang N Y, Shen J Q, Liao P Q, Chen X M, Zhang J P. Hydroxide ligands cooperate with catalytic centers in metal-organic frameworks for efficient photocatalytic CO_2 reduction. Journal of the American Chemical Society, 2018, 140(1): 38-41
9. Lee J S, Won D I, Jung W J, Son H J, Pac C, Kang S O. Widely controllable syngas production by a dye-sensitized TiO_2 hybrid system with Re(I) and Co(III) catalysts under visible-light irradiation. Angewandte Chemie International Edition, 2017, 56(4): 976-980

10. Wang S, Guan B Y, Lu Y, Lou X W D. Formation of hierarchical In_2S_3–$CdIn_2S_4$ heterostructured nanotubes for efficient and stable visible light CO_2 reduction. Journal of the American Chemical Society, 2017, 139(48): 17305-17308
11. Gao C, Meng Q, Zhao K, Yin H, Wang D, Guo J, Zhao S, Chang L, He M, Li Q, et al. Co_3O_4 hexagonal platelets with controllable facets enabling highly efficient visible-light photocatalytic reduction of CO_2. Advanced Materials, 2016, 28(30): 6485-6490
12. Huang C J, Chen C, Zhang M W, Lin L H, Ye X X, Lin S, Antonietti M, Wang X C. Carbon-doped BN nanosheets for metal-free photoredox catalysis. Nature Communications, 2015, 6: 7698